

Article

Study on the Sound Absorption Properties of Recycled Polyester Nonwovens through Alkaline Treatment and Dimple Processing

Gyeong Cheol Yu ¹, Jeong Jin Park ², Eun Hye Kang ¹, Sun Young Lee ³, Youl Huh ⁴ and Seung Goo Lee ^{1,*}

¹ Department of Applied Organic Materials Engineering, Chungnam National University, Daejeon 34134, Republic of Korea

² Department of Organic Materials Engineering, Chungnam National University, Daejeon 34134, Republic of Korea

³ Research Institute for Applied Chemistry and Biological Engineering, Chungnam National University, Daejeon 34134, Republic of Korea; leesy0707@cnu.ac.kr

⁴ Department of Applied Chemistry and Biological Engineering, Graduate School of Industry, Daejeon 34134, Republic of Korea

* Correspondence: lsgoo@cnu.ac.kr; Tel.: +82-42-821-7698

Abstract: This study focused on manufacturing efficient automobile sound-absorbing materials through alkaline treatment and dimple processing of recycled polyethylene terephthalate (rPET) nonwoven fabric. The rPET nonwoven fabric was produced with a sound-absorbing material through compression molding. It was improved through the development of porous sound-absorbing materials through alkaline treatment and resonant sound-absorbing materials through dimple processing. As a result of morphological analysis, alkaline treatment showed that pore size and air permeability increased according to temperature and concentration increase conditions. On the other hand, dimple processing caused a decrease in air permeability and a decrease in pores due to yarn fusion, and as the dimple diameter increased, the sound-absorbing coefficient increased in the 5000 Hz band. Finally, it was judged that effective sound absorption performance would be improved through a simple process through alkaline treatment and dimple processing, and thus there would be applicability in various industrial fields.



Citation: Yu, G.C.; Park, J.J.; Kang, E.H.; Lee, S.Y.; Huh, Y.; Lee, S.G. Study on the Sound Absorption Properties of Recycled Polyester Nonwovens through Alkaline Treatment and Dimple Processing. *Surfaces* **2024**, *7*, 238–250. <https://doi.org/10.3390/surfaces7020016>

Academic Editor: Guido KICKELBICK

Received: 30 January 2024

Revised: 4 March 2024

Accepted: 30 March 2024

Published: 2 April 2024



Copyright: © 2024 by the authors. Licensee MDPI, Basel, Switzerland. This article is an open access article distributed under the terms and conditions of the Creative Commons Attribution (CC BY) license (<https://creativecommons.org/licenses/by/4.0/>).

Keywords: recycled polyethylene terephthalate; sound-absorbing material; alkaline treatment; dimple process; surface modification

1. Introduction

In order to transfer towards sustainable mobility, the automobile industry is currently enhancing the fuel efficiency and eco-friendliness of vehicles by expanding the supply of electric vehicles and incorporating eco-friendly materials and lightweight technology [1,2]. Electric vehicles, lacking an internal combustion engine, eliminate engine and exhaust sounds, creating a serene driving environment [3]. However, friction between the tires and the road surface, collisions of foreign objects between the car's wheel guards and the road surface, and external sounds generate noise in the frequency range of 1 kHz and below, which distracts drivers from focusing on safe driving [4–7]. Consumers are increasingly seeking noise reduction for quiet driving, a notable advantage of electric vehicles. To address these demands, the automobile industry emphasizes the importance of sound-absorbing materials in vehicles. Sound-absorbing materials are actively engaged in technology development to strengthen noise regulations for vehicles progressively and effectively reduce noise levels in vehicles [8,9].

Noise can be reduced by employing sound-absorbing materials to absorb the energy of generated noise, preventing its transmission [10,11]. Sound-absorbing materials play a crucial role in minimizing noise entering the vehicle. These materials are classified into two categories: porous sound-absorbing materials and resonant sound-absorbing

materials, based on their design. Porous sound-absorbing materials consist of numerous micropores, converting incident sound wave energy into thermal energy through the frictional resistance of a skeleton and the air within the pores, effectively dissipating it [12,13]. This type of material is particularly effective in reducing noise in the medium- and high-frequency bands with short wavelengths, displaying the ability to absorb and disperse sounds of various frequencies [14–20]. Resonant sound-absorbing materials, on the other hand, feature a surface structure with multiple small holes, employing the basic principle of the Helmholtz resonator. They absorb sound at specific frequencies by damping due to a pressure difference between external forces and the internal air of the resonant sound-absorbing material [16,21–23].

Sound-absorbing materials include nonwoven fabrics made of fiberglass, felt, polyurethane foam, and vinyl foam [13,24]. However, while these materials are lightweight and functional, they are difficult to recycle or dispose of at the end of their useful life. To address these environmental concerns, polyester nonwovens can be considered as an alternative. PET is, first of all, cost-effective. Second, it is highly recyclable, which can contribute to environmentally friendly carbon reduction. Third, PET is lightweight, strong, and has excellent physical properties and high durability [6,25–29].

Therefore, in this study, we aimed to investigate the effect of physical and chemical processing on the sound absorption performance of rPET nonwovens in order to develop eco-friendly, lightweight and sound-absorbing materials that can be used in the automotive industry to address the transition to sustainable mobility. For this purpose, board-shaped sound-absorbing materials were fabricated using recycled PET nonwovens, and the pores of the nonwovens were increased by alkali processing to make them porous sound-absorbing materials. In addition, a dimple-structured mold was used to change the material into a resonant sound-absorbing material with a dimple structure on the surface through physical processing to improve the sound absorption rate by processing. The sound-absorbing performance was then compared and analyzed [30,31].

2. Materials and Methods

2.1. Materials

In this study, a nonwoven fabric with a sheath–core low-melting-point polyethylene terephthalate (LM PET) staple fiber ($T_m = 70\text{ }^\circ\text{C}$) as a sheath was utilized as a binder for compression molding [32]. The sheath–core LM PET staple fiber and rPET staple fiber, both 4 deniers and 51 mm in length, were provided by Huvis Co., Ltd. (Daejeon, South Korea). These two staple fibers were mixed at a content ratio of 2:8 to prepare a nonwoven fabric through needle punching [33]. Concerning the sound-absorbing material, the nonwoven fabric was cut into $14 \times 14\text{ cm}^2$ pieces, and 10 layers were stacked at $210\text{ }^\circ\text{C}$ and 95 psi for 5 min using a hot press, followed by an additional 20 min of pressurization. Sodium hydroxide pellets (97%, Daejeong Chemical, Jeonbuk, South Korea) and acetic acid (97%, Samchun Chemical, Gyeonggi-do, South Korea) were used as reagents.

2.2. Alkaline Treatment

Alkaline treatment is influenced by the concentration and temperature of the alkaline solution. Therefore, concentration and temperature were considered as variables to assess the effect. The concentrations of the alkaline solution were 10, 15, and 20 *v/v*%, and an aqueous sodium hydroxide solution was prepared using D.I water as a solvent [34]. Subsequently, each solution was used to immerse the sound-absorbing material at 70 and 80 $^\circ\text{C}$ for 60 min. The samples were then taken out and washed with D.I water. After washing, the samples were neutralized with a 5% acetic acid solution and dried at $100\text{ }^\circ\text{C}$ for 3 h in a vacuum dryer. Figure 1 illustrates the surface modification mechanism of recycled PET using alkaline.

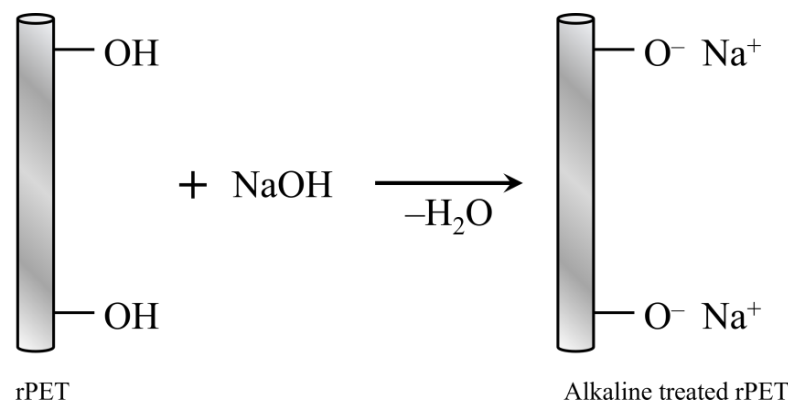


Figure 1. Mechanism of surface modification of rPET using alkaline.

2.3. Dimple-Forming Process

To create a dimpled structure on the surface, protrusions with diameters of 3, 4, and 5 mm were manufactured on a $15 \times 15 \text{ cm}^2$ surface with intervals of 6, 8, and 10 mm, respectively, using a mold with a depth of 2 mm. The lower plate was designed to be flat, allowing the emergence of 1405, 761, and 481 protrusions, respectively.

rPET nonwoven fabric (10 ply) was loaded, heated, and pressed using a hot press at 95 psi and $210 \text{ }^\circ\text{C}$ for 5 min. The material was then cooled for 20 min at room temperature and demolded to produce a resonant sound absorber.

2.4. Measurement of Properties for Sound-Absorbing Material

The thickness of the nonwoven was measured using Vernier calipers (CD-15CP, Mitutoyo, Japan). Measurements were taken three times at different locations and averaged. Weight was determined using a precision balance (Pioneer, Ohaus, Parsippany, NJ, USA) and averaged in triplicate. The weight loss rate was calculated for analysis using Equation (1):

$$\text{Weight loss(\%)} = \frac{W_u - W_t}{W_t} \times 100 \quad (1)$$

where W_u is the weight of the untreated sample and W_t is the weight of the treated sample [35].

An electric field-emission scanning electron microscope (FE-SEM, JSM-7610F, JEOL, Tokyo, Japan) was used to investigate the change in the surface shape resulting from alkaline treatment and dimple processing of the sound-absorbing material. Operating conditions were set to an acceleration voltage of 15 kV and a working distance of 8.4 mm. The alkaline-treated sample was photographed to confirm the change in the macroscopic surface structure and to observe alterations in the fiber surface during alkaline treatment.

The sound-absorbing characteristics of a material are influenced by internal pores [36]. To verify changes in porosity, the unit area and the amount of air passing through per unit time were measured using an automatic air permeability tester (DI-3013, Daelim Starlet, Gyeonggi-do, Siheung, Republic of Korea) according to the ASTM D 737 Fraser method. Samples were manufactured with a size of $17 \times 17 \text{ cm}^2$, and the test was conducted under a pressure condition of 200 Pa.

Furthermore, the pores present on the surface and inside of the sample were analyzed using Brunauer–Emmett–Teller (BET) analysis equipment (ASAPTM 2420, Micromeritics, Norcross, GA, USA). N_2 gas was adsorbed on the sample to assess the changes in pore size and pore volume.

A two-microphone transfer function method with an impression tube kit (type 4206, B&K Company, Nærum, Denmark) was employed to measure the sound absorption coefficient. Pulse analysis software (Pulse version 21) and a spectrum analyzer (type 3560, B&K Company, Nærum, Denmark) were used for sound absorption analysis [37,38]. Figure 2 illustrates the schematic diagram of the impedance tube. After placing each sample on

one side of the impedance tube, the sound absorption coefficient at frequencies ranging from 500 to 6400 Hz was measured by detecting sound reflected from the sample with a microphone, generating noise incident in the vertical direction from the other side.

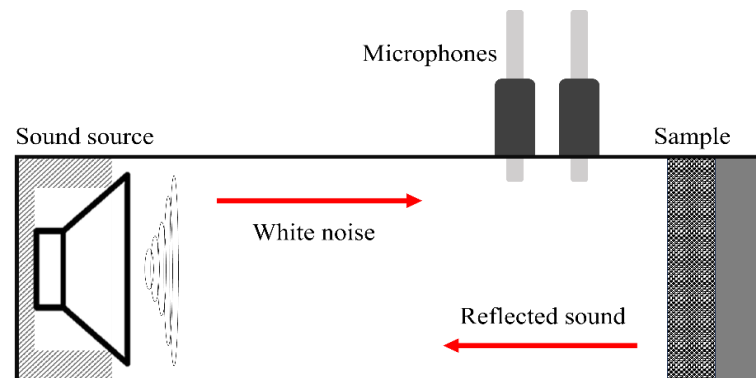


Figure 2. Schematic of the sound absorption coefficient measurement by impedance tube.

3. Results and Discussion

3.1. Rate of Change in Weight and Thickness by Alkaline Treatment

In order to determine the effect of alkaline treatment on the sound-absorbing material sample, the rate of change in weight and thickness was measured based on the concentration and temperature of the alkaline solution, as depicted in Figure 3 and Table 1. It was observed that the weight loss rate of the sound-absorbing material tended to increase with higher concentrations of the alkaline solution, and the rate further increased with elevated temperatures Figure 3a [39]. The change in thickness demonstrated a tendency to decrease with higher concentrations and temperatures of the alkaline solution, similar to the weight loss rate (Figure 3b). The weight loss and thickness reduction of rPET in the alkaline treatment condition of 80 °C temperature and 20% concentration showed a large change compared to other temperature and concentration conditions. Therefore, it can be seen that the alkaline treatment condition of 80 °C temperature and 20% concentration is a harsh environment for rPET.

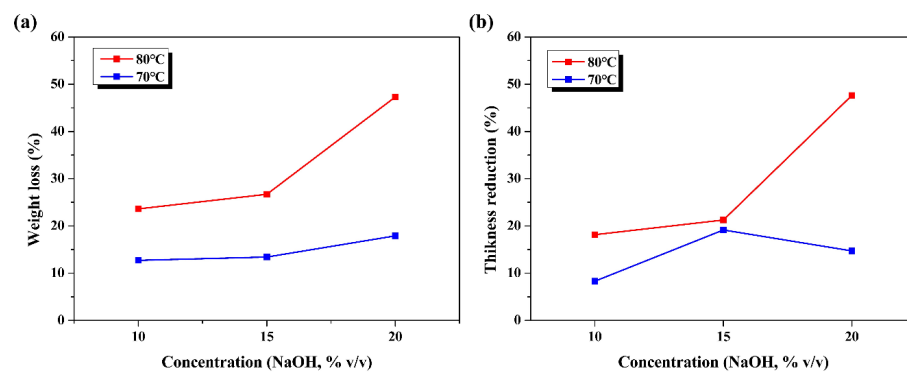


Figure 3. Graphs showing the weight and thickness change rate of recycled sound-absorbing material according to reaction temperature and alkaline concentration during alkaline treatment: (a) weight loss and (b) thickness reduction.

Table 1. Rate of change in weight and thickness under various alkaline treatment conditions.

Treatment Condition		Rate of Change	
Temperature (°C)	NaOH Concentration (v/v%)	Weight Loss (%)	Thickness Reduction (%)
70	10	12.66	8.29
	15	13.40	19.15
	20	26.69	14.70

Table 1. Cont.

Treatment Condition		Rate of Change	
Temperature (°C)	NaOH Concentration (v/v%)	Weight Loss (%)	Thickness Reduction (%)
80	10	17.89	18.15
	15	23.57	21.25
	20	47.33	47.63

The weight loss rate and thickness reduction rate increase as the processing temperature increases. This is because the degree of freedom of rPET increases with increasing temperature, which causes the rPET chains that were not exposed to the surface to be exposed to the fiber surface more often, and the PET chains are attacked by OH ions.

3.2. Analysis of Morphological Changes in Sound-Absorbing Materials during Alkaline Treatment and Dimple Processing

When surface processing is performed, various changes occur on the properties of a sample's surface. Therefore, morphology analysis was conducted to observe alterations in the surface of the sound-absorbing material during alkaline treatment and dimple processing. Figure 4 displays the SEM images of the alkaline-treated sound-absorbing material. When comparing the untreated samples, the fiber diameter of the sample treated at 70 °C with a NaOH concentration of 10% became slightly thinner. It was confirmed that the fiber diameter decreased with NaOH concentrations of 15% and 20%. It can be seen that as the fiber diameter decreases, the pores of the nonwoven fabric widen. In the case of the sample treated at 80 °C with a NaOH concentration of 10%, it was observed that the fibers melted to form a film-like shape. At NaOH concentrations of 15% and 20%, the fibers were observed to have a cut shape, and it can be confirmed that they melted to form a mass. Enormous voids were formed at the NaOH concentration of 20%.

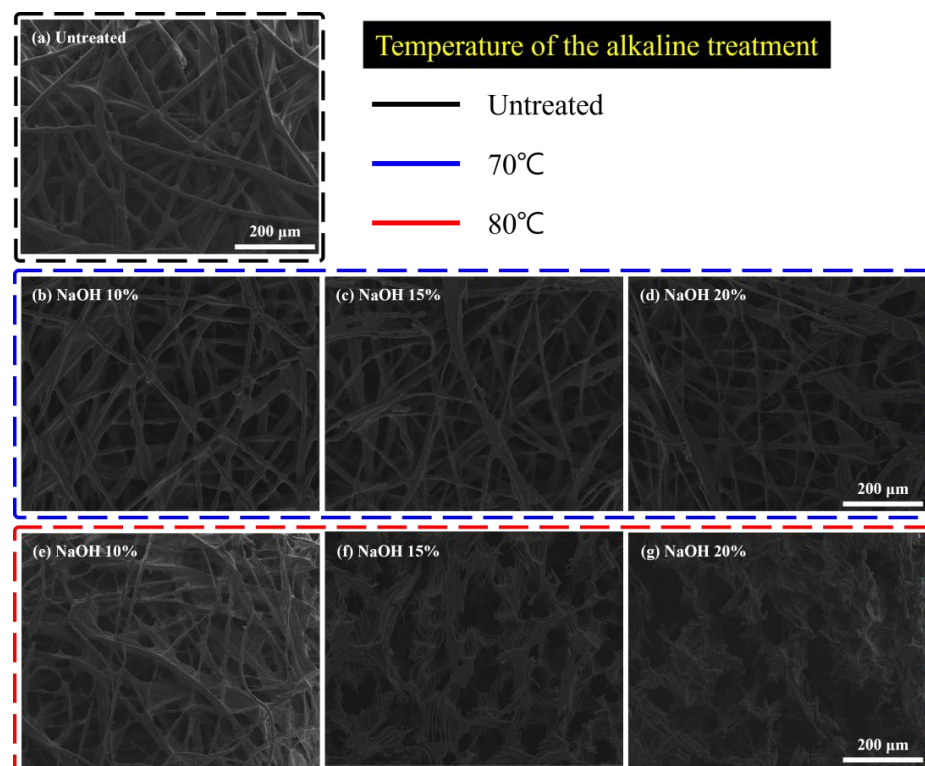


Figure 4. SEM images of the sound-absorbing material, based on the concentration and temperature of the alkaline treatment solution revealed the following conditions: (a) untreated, (b) 70 °C, 10%, (c) 70 °C, 15%, (d) 70 °C, 20%, (e) 80 °C, 10%, (f) 80 °C, 15%, and (g) 80 °C, 20%.

SEM images of the dimple-processed sound-absorbing material are shown in Figure 5. In the sound-absorbing material subjected to the dimple process (Figure 5a–c) at 50× magnification, a fusion of fibers is observed due to the strong pressure applied to the area where the dimple shape is formed compared to other areas during the manufacturing process. In the case of a 3 mm dimple diameter, the smallest dimple shape was observed, whereas for the largest 5 mm diameter, the largest dimple shape was evident. At 250× and 500× magnifications, it was confirmed that the area melted by the fibers increased with the dimple diameter. However, as the dimple diameter increases, the surface area expands, leading to weaker pressure applied to the sound-absorbing material. Therefore, the melting of fibers on the surface was more clearly observed with smaller dimple diameters.

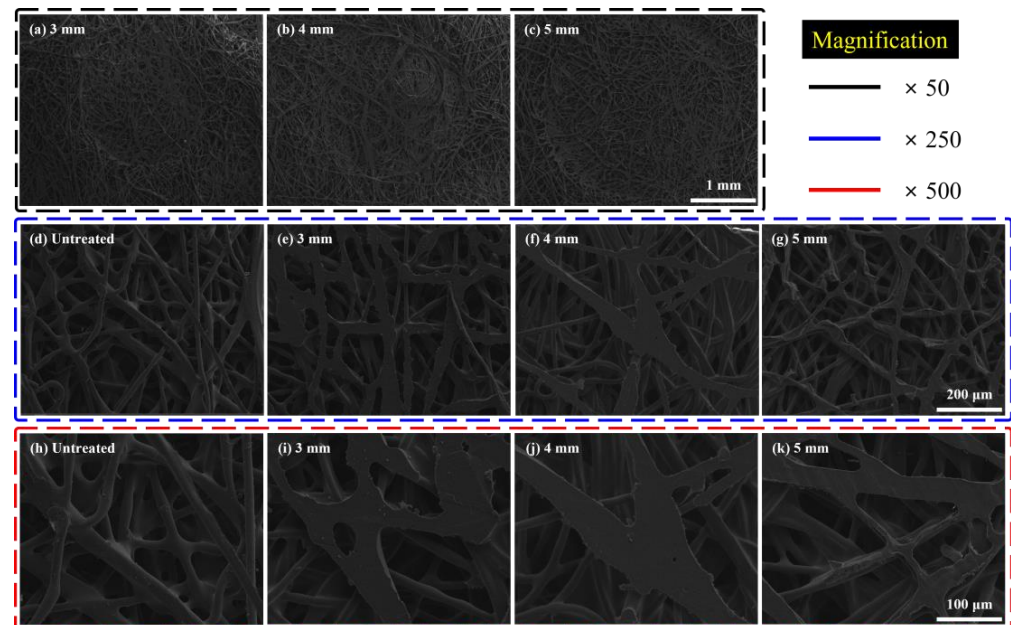


Figure 5. As a result of the surface shape analysis of recycled sound-absorbing materials based on dimple-processing diameter, images at 50×, 250×, and 500× magnifications were obtained for untreated samples, as well as samples with dimple diameters of 3 mm, 4 mm, and 5 mm: (a) 50× of 3 mm, (b) 50× of 4 mm, (c) 50× of 5 mm, (d) 250× of untreated sample, (e) 250× of 3 mm, (f) 250× of 4 mm, (g) 250× of 5 mm, (h) 500× of untreated sample, (i) 500× of 3 mm, (j) 500× of 4 mm, (k) 500× of 5 mm.

3.3. Air Permeability of Alkaline-Treated and Dimple-Processed Sound-Absorbing Materials

The results of the air permeability of the alkaline and dimple-processed samples are shown in Figure 6. The air permeability of the untreated sound-absorbing material was $4.14 \text{ cm}^3/\text{cm}^2/\text{s}$. After alkaline treatment, the overall air permeability increased (Figure 6a). At the lowest solution concentration of 10% and a temperature of $70 \text{ }^\circ\text{C}$, it showed an air permeability of $7.94 \text{ cm}^3/\text{cm}^2/\text{s}$, approximately twice that of the untreated sample. Additionally, as the alkaline treatment concentration and temperature increased, the air permeability gradually increased. It was observed that the air permeability rapidly increased under the harshest environment at NaOH concentration of 20% and treatment temperature at $80 \text{ }^\circ\text{C}$ [40].

The air permeability results for the dimple-processed sound-absorbing material are given in Figure 6b. The sound-absorbing material processed with a 3 mm dimple diameter exhibited $3.00 \text{ cm}^3/\text{cm}^2/\text{s}$, the 4 mm dimple-processed sound-absorbing material showed $3.35 \text{ cm}^3/\text{cm}^2/\text{s}$, and the 5 mm dimple-processed sound-absorbing material exhibited $3.76 \text{ cm}^3/\text{cm}^2/\text{s}$. These values indicated reduced air permeability compared to the untreated sound-absorbing material. The decrease in air permeability for the dimple-processed sound-absorbing material is attributed to the reduction in surface pores due

to yarn fusion in the dimple-shaped region, causing airflow disruptions and reducing air permeability.

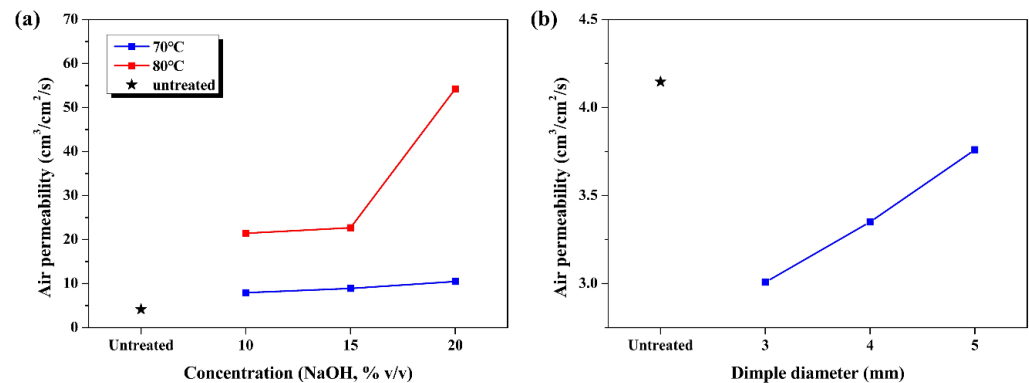


Figure 6. Graphs depicting the rate of change in air permeability by (a) the alkaline-treated samples and (b) the dimple-processed samples.

3.4. Adsorption and Desorption Pore Volume Changes of Sound-Absorbing Materials with Alkaline Treatment

The changes in pore volume of the sound-absorbing material prepared by alkaline treatment were analyzed by comparing them with the untreated sample. The pore volume changes during adsorption and desorption of sound-absorbing materials are shown in Figure 7. Figure 7a shows the changes in pore volume during adsorption with respect to the change in pore diameter, while Figure 7b shows changes in pore volume during desorption with the change in pore diameter. The pore volume during both adsorption and desorption generally increased as the pore diameter increased. Additionally, the pore volume during both of the processes increased with higher concentrations and temperatures of alkaline treatment. This suggests that the pore volume increases as the pore size of the sound-absorbing material increases through alkaline treatment.

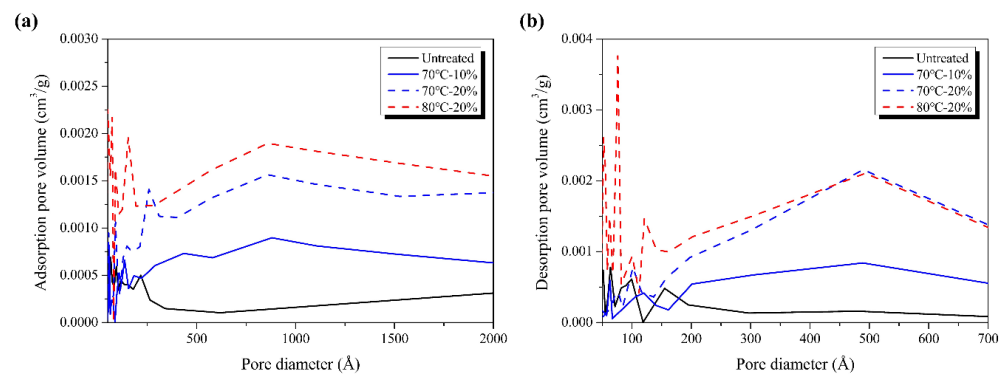
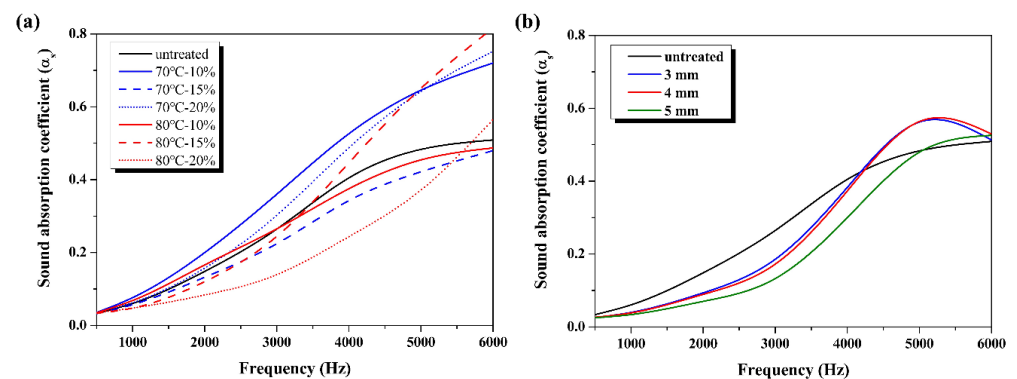


Figure 7. Changes in pore volume of alkaline-treated sound-absorbing materials: (a) adsorption pore volume sample and (b) desorption pore volume sample.

In addition, in general, materials with a large pore volume exhibit high sound absorption. This is because if the pore volume is large, there is more space where sound can enter the material, scatter, and be absorbed [41]. The cumulative adsorption volume of pores of the untreated and alkaline-treated samples are compared and shown in Table 2. Compared with the untreated sample, the sample with a treatment temperature of 80 °C and NaOH concentration of 15% and the sample with a treatment temperature of 70 °C and NaOH concentration of 20% showed the largest volume change. It can be seen from Figure 8 that the sound absorption of this alkaline-treated sample is improved compared to that of the untreated sample.

Table 2. Cumulative adsorption volume of samples treated with alkaline and untreated samples.

Treatment Condition		Volume of Pores of Change
Temperature (°C)	NaOH Concentration (v/v%)	Adsorption Cumulative Volume of Pores (cm ³ /g)
0	0	0.00058
70	10	0.00174
	15	0.00093
	20	0.00205
80	10	0.00145
	15	0.00366
	20	0.00152

**Figure 8.** Sound absorption coefficients of recycled sound-absorbing materials through (a) the alkaline-treated sample and (b) the dimple-processed sample.

3.5. Changes in the Sound Absorption Coefficients of Alkaline-Treated and Dimple-Processed Sound-Absorbing Materials

To analyze the sound absorption characteristics of the porous sound-absorbing material manufactured through alkaline treatment and the resonant sound-absorbing material manufactured through dimple processing, the change in the sound absorption rate was analyzed compared to the untreated sample. Figure 8 shows the results of changes in the sound absorption coefficients of the alkaline-treated and dimple-processed recycled sound-absorbing material.

In Figure 8a, the untreated sound-absorbing material exhibits an increase from a low-frequency region to a medium-frequency region, followed by a gradual rise in the high-frequency region. The sound-absorbing material treated with NaOH concentration of 10% and treatment temperature of 70 °C showed the most significant increase in the sound absorption rate across the entire frequency range compared to the untreated sound-absorbing material. In particular, there was a substantial increase in the high-frequency range of 3000 Hz or more. However, under NaOH concentration of 20% and treatment temperature of 80 °C treatment conditions, the sound absorption rate tended to decrease, rather than matching the untreated sample. There was no distinct trend in the sound absorption rate change due to the reduction caused by alkaline treatment. However, it was observed that the alkaline-treated sample improved compared to the untreated sample, but the sample in the harsh alkaline treatment environment decreased the sound absorption rate compared to the untreated sample. Therefore, the weight and thickness, important factors affecting the sound absorption rate, also change simultaneously, and it is believed to have been greatly affected by this.

Figure 8b shows the change in the sound absorption rate according to the dimple shape. The untreated sample without shape exhibited the highest sound absorption rate at low frequencies, with a slightly lower sound absorption rate at high frequencies of 4000 Hz or more. There was a difference in the change in sound absorption rate according to the

diameter of the dimple shape. It was confirmed that the sound absorption rate of the samples with a diameter of 3 mm and 4 mm decreased at low frequencies compared to the untreated sample, and sound absorption performance was improved at a high frequency of 4000 Hz or more. In the case of the sound absorption rate of a sample with a diameter of 5 mm, compared to the untreated sample, the sound absorption performance was improved at a high frequency of 5000 Hz or more. In conclusion, it was also confirmed that the dimple structure formed on the surface exhibited the same characteristics as the resonant sound-absorbing material, and the resonant sound-absorbing material also showed excellent sound absorption performance at a specific frequency. In the case of a dimple-processed sample, the sound absorption performance was greatly improved at 4000–6000 Hz.

In order to confirm the sound absorption improvement effect of the alkaline treatment, sound absorption characteristics were compared between the sample reduced by alkaline treatment and a comparative sample with the same weight. Therefore, the sound absorption rate was compared by preparing a sound absorption material with a weight similar to the reduced sample by adjusting the ply layers of the sound absorption material. Figure 9 shows the improved sample and the sound absorption rate based on the sample produced by changing the weight under different conditions of the number of ply.

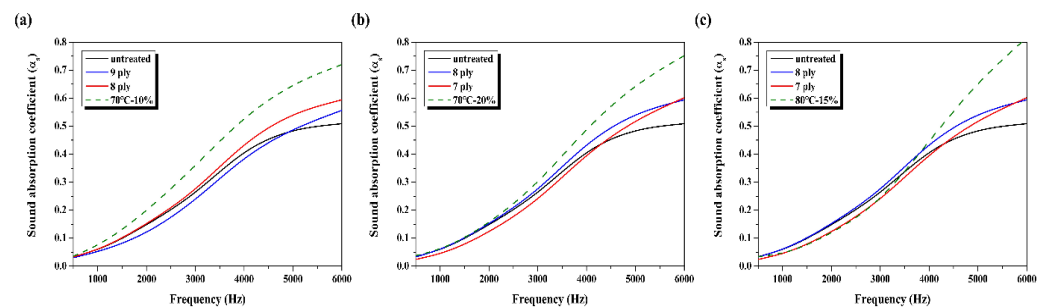


Figure 9. Comparing the sound absorption coefficient between the reduced sample through alkaline treatment and the sample with similar weight by controlling the fly water: (a) NaOH 10% 70 °C (loss in weight 12.7%), (b) NaOH 20% 70 °C (loss in weight 26.7%) and (c) NaOH 15% 80 °C (loss in weight 23.7%).

Figure 9a shows the comparison of the sound absorption rates of samples treated under the temperature conditions of 70 °C (12.7% loss in weight), 9 ply (10% loss in weight), and 8 ply (20% loss in weight) in a 10% NaOH aqueous solution. The sample treated under the condition of 70 °C in 10% NaOH solution showed a high sound absorption rate in the overall frequency domain compared to the untreated sample, 9 ply (10% loss in weight), and 8 ply (20% loss in weight).

Figure 9b shows the comparison of the sound absorption rates of samples treated under conditions of 70 °C (26.7% loss in weight), 8 ply (20% loss in weight), and 7 ply (30% loss in weight) in a 20% NaOH aqueous solution. Samples at a temperature of 70 °C in a 20% NaOH aqueous solution did not differ significantly from other samples in the frequency range of 2000 Hz or less, but they showed a slight improvement in the sound absorption rate in the frequency range of 2000 Hz or more, and it was confirmed that the sound absorption rate increased significantly in the range of 3000 Hz or more.

Figure 9c shows the comparison of the sound absorption rates of samples treated under the conditions of 80 °C (23.7% loss in weight), 8 ply (20% loss in weight), and 7 ply (30% loss in weight) in a 15% NaOH aqueous solution. A sample at a temperature of 80 °C showed a similar sound absorption rate below 4000 Hz when comparing the sound absorption rate with the untreated sample, 9 ply (10% loss in weight), and 8 ply (20% loss in weight), but it was confirmed that the sound absorption performance was significantly improved in the area of 4000 Hz or more compared to other samples.

In order to control the effect of the thickness of the sample on the sound absorption property and to compare only the effect of alkaline treatment on the sound absorption

property of a sample of the same thickness, the sound absorption rate divided by the thickness of the sample was calculated and replotted, as shown in Figure 10. The sound absorption coefficient of the untreated sample was the lowest in the entire frequency range. In the frequency range below 2000 Hz, the sound absorption rate of samples treated with alkaline tended to slightly increase. The sound absorption rate of the sample treated at temperature of 70 °C and concentration of 10% was highest, but there was little difference by treatment condition. In the 2000–4000 Hz frequency band, the sound absorption rate of the sample tended to increase further with alkaline treatment.

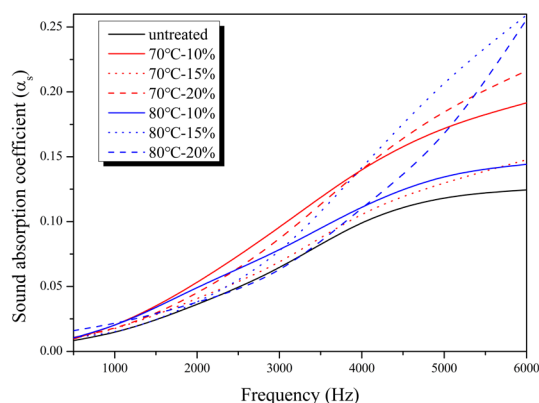


Figure 10. Thickness-normalized sound absorption coefficients of recycled sound-absorbing materials.

However, in the 4000–5000 Hz frequency band, the sound absorption coefficient of the sample treated at a temperature of 80 °C and concentration of 15% and the sample treated at a temperature of 70 °C and concentration of 20% increased more than that of the sample treated at a temperature of 70 °C and concentration of 10%. In the frequency band above 5000 Hz, the sound absorption coefficient of the sample treated at temperature of 80 °C and concentration of 15%, the sample treated at temperature of 80 °C and concentration of 20%, and the sample treated at temperature of 70 °C and concentration of 20% increased more than that of the treated sample treated at a temperature of 70 °C and a concentration of 10%.

These results are believed to have improved the sound absorption rate in the high-frequency range above 4000 Hz because the pore diameter and pore volume of the rPET nonwoven fabrics increased when the alkaline treatment conditions were intensified.

4. Conclusions

This study aimed to develop a lightweight sound-absorbing material that enhances sound-absorbing performance using eco-friendly materials. This was achieved by manufacturing a sound-absorbing material through thermal compression molding of rPET nonwoven fabric and applying dimple processing and a chemical method. The goal was to create a lightweight material with improved sound-absorbing performance, harnessing the porous characteristics of rPET nonwoven fabric and resonant sound-absorbing characteristics through dimple processing, with variations in alkaline treatment conditions. The results of the comparison and analysis of sound-absorbing performance and characteristics of the nonwoven fabric under different alkaline treatment conditions and dimple structures are presented below.

Through alkaline treatment, reforming, and dehydration, reactions occur on the surface of rPET, leading to changes in weight and thickness. Regarding the alterations in weight and thickness, it was observed that both decreased under severe alkaline treatment conditions. Specifically, the weight and thickness exhibited a notable reduction in environmental conditions characterized by higher concentrations and temperatures of the NaOH aqueous solution. The most significant decrease occurred at 80 °C under 20% concentration of the harsh NaOH aqueous solution.

In addition, it was confirmed that the volume of the changed pores through the alkali treatment was related to the degree of sound absorption. The sample at a temperature of

80 °C and with a concentration of 15% and the sample at a temperature of 70 °C and with a concentration of 20% showed a large volume change. In addition, it was confirmed that the sample treated under these conditions improved when compared to the sample without treatment in terms of the degree of sound absorption.

When observing the surface shapes of the alkaline-treated and dimple-processed samples, it was evident that the thickness of the yarn in the sound-absorbing material, which significantly decreased in the alkaline-treated sample, reduced and the surface pores of the nonwoven fabric increased. The dimple-processed sample applied higher pressure to the dimple-processing area, leading to the fusion of the yarn and resulting in a film-shaped surface.

As a result of measuring the sound absorption coefficient of the specimens under each alkaline treatment condition in the frequency band of 500–6000 Hz, it was observed that compared to the untreated sample without alkaline treatment, the sound absorption coefficient of the specimens under the conditions of 70 °C in 10% and 20% NaOH aqueous solution and 80 °C in 15% NaOH aqueous solution increased across the entire frequency range. The sound absorption coefficient further increased in the range of 5500 Hz or more under the condition of 80 °C in a 20% NaOH aqueous solution. It was confirmed that the sound absorption performance was influenced by the complex changes in the shape, weight, and thickness of the pores resulting from alkaline treatment.

In the case of specimens subjected to dimple processing under diameter conditions of 3 mm, 4 mm, and 5 mm, the sound absorption coefficient decreased in the low- and medium-frequency bands but increased in the frequency range of 5000 Hz or more. The sound absorption characteristics of the resonant sound-absorbing material manifested in the frequency range of 5000 Hz or more, and the smaller the dimple diameter, the better the expression of resonant sound absorption characteristics.

Through this study, it was confirmed that the sound-absorbing properties of a material against noise generated in a high-frequency domain were improved by using alkaline treatment and dimple processing. This economical and straightforward process can be expected to reduce high-frequency noise generated from friction between the road surface and wheels when driving an electric vehicle. Additionally, it can provide a comfortable driving experience for drivers through postprocessing of the wheel guard that is currently commercially available.

However, further research is needed to explore reuse options and prevent environmental problems caused by alkali during the weight loss process.

Author Contributions: Conceptualization, Y.H. and S.Y.L.; methodology, J.J.P., Y.H. and S.Y.L.; validation, G.C.Y. and J.J.P.; formal analysis, G.C.Y.; investigation, G.C.Y., J.J.P. and E.H.K.; resources, G.C.Y. and J.J.P.; data curation, G.C.Y.; writing—original draft preparation, G.C.Y., J.J.P. and S.Y.L.; writing—review and editing, G.C.Y., J.J.P. and S.Y.L.; visualization, G.C.Y.; supervision, S.G.L.; project administration, S.G.L.; funding acquisition, S.G.L. All authors have read and agreed to the published version of the manuscript.

Funding: This work was supported by the Technology Innovation Program (1415185366) funded by the Ministry of Trade, Industry and Energy (MOTIE, Republic of Korea).

Institutional Review Board Statement: Not applicable.

Informed Consent Statement: Not applicable.

Data Availability Statement: The data presented in this study are available in this article.

Conflicts of Interest: The authors declare no conflicts of interest.

References

1. Kumar, R.R.; Alok, K. Adoption of Electric Vehicle: A Literature Review and Prospects for Sustainability. *J. Clean. Prod.* **2020**, *253*, 119911. [[CrossRef](#)]
2. Adu-Gyamfi, G.; Asamoah, A.N.; Obuobi, B.; Nketiah, E.; Zhang, M. Electric Mobility in an Oil-Producing Developing Nation: Empirical Assessment of Electric Vehicle Adoption. *Technol. Forecast. Soc. Change* **2024**, *200*, 123173. [[CrossRef](#)]

3. Huang, H.B.; Wu, J.H.; Huang, X.R.; Ding, W.P.; Yang, M.L. A Novel Interval Analysis Method to Identify and Reduce Pure Electric Vehicle Structure-Borne Noise. *J. Sound Vib.* **2020**, *475*, 115258. [[CrossRef](#)]
4. Hua, X.; Thomas, A.; Shultis, K. Recent Progress in Battery Electric Vehicle Noise, Vibration, and Harshness. *Sci. Prog.* **2021**, *104*, 00368504211005224. [[CrossRef](#)] [[PubMed](#)]
5. Palak, H.; Karagüzel Kayaoğlu, B. Analysis of the Effect of Production Parameters on Sound Absorption and Abrasion Resistance Performance of Needle-punched Nonwovens for Automotive Carpet Applications Using Taguchi Method. *J. Ind. Text.* **2021**, *51*, 714–739. [[CrossRef](#)]
6. Liu, Z.; Fard, M.; Davy, J.L. Prediction of the Acoustic Effect of an Interior Trim Porous Material inside a Rigid-Walled Car Air Cavity Model. *Appl. Acoust.* **2020**, *165*, 107325. [[CrossRef](#)]
7. Del Pizzo, L.G.; Teti, L.; Moro, A.; Bianco, F.; Fredianelli, L.; Licitra, G. Influence of Texture on Tyre Road Noise Spectra in Rubberized Pavements. *Appl. Acoust.* **2020**, *159*, 107080. [[CrossRef](#)]
8. Singh, S.; Mohanty, A.R. HVAC Noise Control Using Natural Materials to Improve Vehicle Interior Sound Quality. *Appl. Acoust.* **2018**, *140*, 100–109. [[CrossRef](#)]
9. Wang, Z.; Li, P.; Liu, H.; Yang, J.; Liu, S.; Xue, L. Objective Sound Quality Evaluation for the Vehicle Interior Noise Based on Responses of the Basilar Membrane in the Human Ear. *Appl. Acoust.* **2021**, *172*, 107619. [[CrossRef](#)]
10. Ghorbani, K.; Hasani, H.; Zarrebini, M.; Saghafi, R. An Investigation into Sound Transmission Loss by Polypropylene Needle-Punched Nonwovens. *Alex. Eng. J.* **2016**, *55*, 907–914. [[CrossRef](#)]
11. Chen, J.; Li, H.; Yan, Z.; Zhang, Z.; Gong, J.; Guo, Y.; Zhang, J. Simulation, Measurement and Optimization of Sound Absorption in Gradient Impedance Fiber-Based Composites. *Measurement* **2023**, *221*, 113499. [[CrossRef](#)]
12. Cao, L.; Fu, Q.; Si, Y.; Ding, B.; Yu, J. Porous Materials for Sound Absorption. *Compos. Commun.* **2018**, *10*, 25–35. [[CrossRef](#)]
13. Sharma, S.; Sudhakara, P.; Singh, J.; Singh, S.; Singh, G. Emerging Progressive Developments in the Fibrous Composites for Acoustic Applications. *J. Manuf. Process.* **2023**, *102*, 443–477. [[CrossRef](#)]
14. Yang, T.; Hu, L.; Xiong, X.; Petru, M.; Noman, M.T.; Mishra, R.; Militký, J. Sound Absorption Properties of Natural Fibers: A Review. *Sustainability* **2020**, *12*, 8477. [[CrossRef](#)]
15. Zhang, W.; Liu, X.; Xin, F. Sound Absorption Performance of Helically Perforated Porous Metamaterials at High Temperature. *Mater. Des.* **2023**, *225*, 111437. [[CrossRef](#)]
16. Liu, X.; Yu, C.; Xin, F. Gradually Perforated Porous Materials Backed with Helmholtz Resonant Cavity for Broadband Low-Frequency Sound Absorption. *Compos. Struct.* **2021**, *263*, 113647. [[CrossRef](#)]
17. Kim, B.S.; Park, J. Double Resonant Porous Structure Backed by Air Cavity for Low Frequency Sound Absorption Improvement. *Compos. Struct.* **2018**, *183*, 545–549. [[CrossRef](#)]
18. Dunne, R.; Desai, D.; Sadiku, R. A Review of the Factors That Influence Sound Absorption and the Available Empirical Models for Fibrous Materials. *Acoust. Aust.* **2017**, *45*, 453–469. [[CrossRef](#)]
19. Li, X.; Liu, B.; Wu, Q. Enhanced Low-Frequency Sound Absorption of a Porous Layer Mosaicked with Perforated Resonator. *Polymers* **2022**, *14*, 223. [[CrossRef](#)]
20. Huang, H.; Lim, T.C.; Wu, J.; Ding, W.; Pang, J. Multitarget Prediction and Optimization of Pure Electric Vehicle Tire/Road Airborne Noise Sound Quality Based on a Knowledge- and Data-Driven Method. *Mech. Syst. Signal Process* **2023**, *197*, 110361. [[CrossRef](#)]
21. Kalinova, K. Sound Absorptive Light Comprising Nanofibrous Resonant Membrane Applicable in Room Acoustics. *Build. Serv. Eng. Res. Technol.* **2018**, *39*, 362–370. [[CrossRef](#)]
22. Yang, D.; Wang, X.; Zhu, M. The Impact of the Neck Material on the Sound Absorption Performance of Helmholtz Resonators. *J. Sound Vib.* **2014**, *333*, 6843–6857. [[CrossRef](#)]
23. Liu, Q.; Liu, X.; Zhang, C.; Xin, F. A Novel Multiscale Porous Composite Structure for Sound Absorption Enhancement. *Compos. Struct.* **2021**, *276*, 114456. [[CrossRef](#)]
24. Yang, T.; Mishra, R.; Horoshenkov, K.V.; Hurrell, A.; Saati, F.; Xiong, X. A Study of Some Airflow Resistivity Models for Multi-Component Polyester Fiber Assembly. *Appl. Acoust.* **2018**, *139*, 75–81. [[CrossRef](#)]
25. Shao, X.; Yan, X. Sound Absorption Properties of Nanofiber Membrane-Based Multi-Layer Composites. *Appl. Acoust.* **2022**, *200*, 109029. [[CrossRef](#)]
26. Miller, L.; Soulliere, K.; Sawyer-Beaulieu, S.; Tseng, S.; Tam, E. Challenges and Alternatives to Plastics Recycling in the Automotive Sector. *Materials* **2014**, *7*, 5883–5902. [[CrossRef](#)] [[PubMed](#)]
27. Watanabe, K.; Minemura, Y.; Nemoto, K.; Sugawara, H. Development of High-Performance All-Polyester Sound-Absorbing Materials. *JSAE Rev.* **1999**, *20*, 357–362. [[CrossRef](#)]
28. Yao, Z.; Cai, J.; Wang, X.; Yang, Y.; He, Y. Application of Equivalent Diameter in Sound Absorption Performance Prediction of Non-Circular Sectional Polyester Fibers. *Appl. Acoust.* **2021**, *182*, 108238. [[CrossRef](#)]
29. Volpe, V.; Lanzillo, M.S.; Molaro, A.; Affinita, G.; Pantani, R. Characterization of Recycled/Virgin Polyethylene Terephthalate Composite Reinforced with Glass Fiber for Automotive Applications. *J. Compos. Sci.* **2022**, *6*, 59. [[CrossRef](#)]
30. Rutkevičius, M.; Austin, Z.; Chalk, B.; Mehl, G.H.; Qin, Q.; Rubini, P.A.; Stoyanov, S.D.; Paunov, V.N. Sound Absorption of Porous Cement Composites: Effects of the Porosity and the Pore Size. *J. Mater. Sci.* **2015**, *50*, 3495–3503. [[CrossRef](#)]
31. Wang, W.; Liu, H.; Gu, W. A Novel Fabrication Approach for Improving the Mechanical and Sound Absorbing Properties of Porous Sound-Absorbing Ceramics. *J. Alloys Compd.* **2017**, *695*, 2477–2482. [[CrossRef](#)]

32. Kim, K.Y.; Doh, S.J.; Im, J.N.; Jeong, W.Y.; An, H.J.; Lim, D.Y. Effects of Binder Fibers and Bonding Processes on PET Hollow Fiber Nonwovens for Automotive Cushion Materials. *Fibers Polym.* **2013**, *14*, 639–646. [[CrossRef](#)]
33. Sivri, Ç.; Haji, A. Surface Coating of Needle-Punched Nonwovens with Meltblown Nonwovens to Improve Acoustic Properties. *Coatings* **2022**, *12*, 1092. [[CrossRef](#)]
34. Čorak, I.; Tarbuk, A.; Đorđević, D.; Višić, K.; Botteri, L. Sustainable Alkaline Hydrolysis of Polyester Fabric at Low Temperature. *Materials* **2022**, *15*, 1530. [[CrossRef](#)]
35. Chen, T.; Zhang, W.; Zhang, J. Alkali Resistance of Poly(Ethylene Terephthalate) (PET) and Poly(Ethylene Glycol-Co-1,4-Cyclohexanedimethanol Terephthalate) (PETG) Copolyesters: The Role of Composition. *Polym. Degrad. Stab.* **2015**, *120*, 232–243. [[CrossRef](#)]
36. Kalauni, K.; Pawar, S.J. A Review on the Taxonomy, Factors Associated with Sound Absorption and Theoretical Modeling of Porous Sound Absorbing Materials. *J. Porous Mater.* **2019**, *26*, 1795–1819. [[CrossRef](#)]
37. Kim, H.S.; Ma, P.S.; Kim, B.K.; Kim, S.R.; Lee, S.H. Near-Field Effects on the Sound Transmission and Absorption of Elastic Micro-Perforated Plates in Impedance Tubes. *J. Sound Vib.* **2021**, *499*, 116001. [[CrossRef](#)]
38. Corredor-Bedoya, A.C.; Acuña, B.; Serpa, A.L.; Masiero, B. Effect of the Excitation Signal Type on the Absorption Coefficient Measurement Using the Impedance Tube. *Appl. Acoust.* **2021**, *171*, 107659. [[CrossRef](#)]
39. Kumagai, S.; Hirahashi, S.; Grause, G.; Kameda, T.; Toyoda, H.; Yoshioka, T. Alkaline Hydrolysis of PVC-Coated PET Fibers for Simultaneous Recycling of PET and PVC. *J. Mater. Cycles Waste Manag.* **2018**, *20*, 439–449. [[CrossRef](#)]
40. Youn, S.; Hee Park, C. Development of Breathable Janus Superhydrophobic Polyester Fabrics Using Alkaline Hydrolysis and Blade Coating. *Text. Res. J.* **2019**, *89*, 959–974. [[CrossRef](#)]
41. Soltani, P.; Norouzi, M. Prediction of the Sound Absorption Behavior of Nonwoven Fabrics: Computational Study and Experimental Validation. *J. Sound Vib.* **2020**, *485*, 115607. [[CrossRef](#)]

Disclaimer/Publisher’s Note: The statements, opinions and data contained in all publications are solely those of the individual author(s) and contributor(s) and not of MDPI and/or the editor(s). MDPI and/or the editor(s) disclaim responsibility for any injury to people or property resulting from any ideas, methods, instructions or products referred to in the content.